Applied Catalysis B: Environmental 305 (2022) 121051

Contents lists available at ScienceDirect

Applied Catalysis B: Environmental

journal homepage: www.elsevier.com/locate/apcatb

Hydrothermal process assisted by photocatalysis: Towards a novel hybrid mechanism driven glucose valorization to levulinic acid, ethylene and hydrogen

Insaf Abdouli *, Frederic Dappozze, Marion Eternot, Nadine Essayem, Chantal Guillard

University Lyon, University Claude Bernard, CNRS, IRCELYON, UMR5256, Villeurbanne 69626, France

ARTICLE INFO

Keywords:
Ethylene
Hydrogen
Hydrothermal process assisted by photocatalysis
Levulinic acid
Titanium dioxide

ABSTRACT

The effect of UV irradiation on titanium dioxide catalyzed glucose conversion in value added molecules was studied at high temperatures, 120–150 °C, in anaerobic conditions. The reaction was implemented in a batch reactor designed to combine high temperature/pressure and irradiation. Inhibition of the titanium dioxide catalytic performances to produce gluconic acid was observed upon UV irradiation which allows the selective formation of levulinic acid in high yield, ~ 60% at 150 °C, together with the co-production of ethylene and hydrogen in the gas phase. The formation of levulinic acid could be explained by the creation of Brønsted acidity in the reaction medium upon irradiation. The reasons of this phenomenon are discussed considering that UV could modify the electronic properties of titanium dioxide by electron-holes pairs formation and the possible H^+ promotion.

1. Introduction

Bio-based chemicals production from biomass resources has been widely investigated to substitute fossil resources. 12 biobased molecules have been selected by the US Department of Energy as building blocks or platform chemicals: xylitol, sorbitol, 3-hydroxybutyrolactone, glutamic acid, glycerol, itaconic acid, aspartic acid, 3-hydroxy propionic acid, glucaric acid, 2,5-furan dicarboxylic acid, succinic acid and levulinic acid [1]. Those molecules production has been studied starting from lignocellulosic biomass or from its major components: monosaccharides (glucose, xylose…) under different process conditions (temperature, pressure, solvent, catalyst…).

Levulinic acid is a platform molecule due to its reactive carbonyl and carboxylic groups that allow its transformation into a wide range of chemicals (methyltetrahydrofuran, valerolactone…), fuel additives (Butyl levulinates [2]), and polymer materials [1]. Its production is well established at the commercial scale by the Biofine process based on H_2SO_4 catalyzed carbohydrates dehydration at 190–200 °C [3]. The process achieves levulinic acid yield of ~ 50 wt% and formic acid yields of 20 wt% from hexoses. Only strong mineral acid such as H_2SO_4 or HCl catalyzes efficiently the direct conversion of glucan or glucose into levulinic acid and formic acid while less corrosive solid acid catalysts such as H-ZSM5 present generally a lower activity than H_2SO_4 [4]. Among the few articles dealing with heterogeneously catalyzed hexoses conversion into levulinic acid [5,6], Nb based mesoporous oxide was found to give a relatively high levulinic acid yield, of 64%, from glucose at 180 °C in 3 h. It is generally accepted that the mechanism of hexoses conversion into levulinic acid proceeds via the well know intermediate, 5-hydroxymethylfurfural (5-HMF) obtained from fructose dehydration by a Brønsted acid catalyzed step [7,8] which is further rehydrated over the same type of acid catalyst to form levulinic acid and formic acid [9,10]. When glucose is used as feedstock, the use of Lewis acid [10,11] and/or basic catalyst [12,13] is often necessary to isomerize first glucose into fructose, fructose being much more rapidly dehydrated into 5-HMF than glucose.

Ethylene is another interesting platform molecule that is a very reactive gas conventionally obtained by cracking petroleum [13,14]. It is the most produced organic molecule in the world used in many fields such as for polyethylene (PET) production. But the cracking process is high energy consuming [15] and high CO_2 emitter [14]. So, developing new less energy consuming and less pollutant processes to produce ethylene received significant attention. Ethylene production has been largely studied from ethanol by dehydration in presence of acid catalysts as an alternative for cracking process [15–19]. This transformation is

* Corresponding author.
E-mail address: insaf.abdouli@ireclyon.univ-lyon1.fr (I. Abdouli).

https://doi.org/10.1016/j.apcatb.2021.121051
Received 7 September 2021; Received in revised form 27 December 2021; Accepted 28 December 2021
Available online 4 January 2022

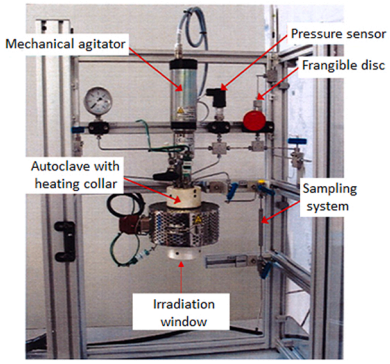

Fig. 1. Used reactor.

ethylene selective at high temperature [18]. Ethanol dehydration in gas phase produces almost 100% ethylene at temperatures higher than 190 °C [15,17–19]. For example, Chen et al. achieved a selectivity of 100% in ethylene in presence of TiO_2/Al_2O_3, only at temperatures higher than 440 °C [20] or at lower temperatures, ~ 300 °C over H-ZSM-5 [21]. Ethylene was also obtained by photocatalytic degradation, at ambient temperature, of acrylic and propionic acids but in very low quantities [22]. Photocatalysis is a low energy consuming process. In fact, it is generally conducted under ambient temperature and atmospheric pressure to mineralize pollutants [23,24] and more recently to produce hydrogen from biomass [25,26].

Hydrogen has been attracting attention as energy vector. Actually, it is mostly produced from fossil resources (coal, oil and natural gas) with CO_2 as by-product [25–27]. Because of environmental concerns and fossil resources depletion, many efforts have been made to produce hydrogen by low carbon emitter processes for energy use (mobility…). In this context, due to its low energy consumption, photocatalysis appears as a promising process to produce hydrogen from a variety of substrates such as alcohols [27] and biomass derivates (cellulose, carbohydrates) [25,28–31] in presence of different photocatalysts. The most used photocatalysts are based on noble metals (Au, Pt, Pd…) supported on titanium dioxide [25,30,31].

Thus, in this work, the production of those two platform molecules (levulinic acid and ethylene) together with hydrogen was studied from glucose in presence of commercial titanium dioxide catalysts (TiO_2) by an innovative process. This novel process consists in the combination of hydrothermal and photocatalytic processes. Combined and separated processes were compared to show the combination contribution. They were performed in the same reactor and under the same conditions of atmosphere, pressure, volume, stirring and glucose-catalyst concentrations.

2. Materials and methods

2.1. Materials

Glucose was purchased from Merck and all the chemicals used for the calibration with HPLC were purchased from Aldrich.

For this study, two commercial titanium dioxide catalysts were used: a pure anatase (UV100: 300 $m^2\ g^{-1}$) from Sachtleben Chemie and a pure rutile (Rut160: 175 $m^2\ g^{-1}$) from Nanostructured and Amorphous Materials Incorporation. Rut160 was pretreated for 20 h at 400 °C under air before use to remove carbon pollution. Rut160 also contains Si (5 wt%).

2.2. Glucose valorization

Glucose valorization was studied by hydrothermal and photocatalytic combined process and by each separated one in the same reactor. The reactor is a stainless-steel autoclave equipped with a glass window in its bottom allowing to work under irradiation, high temperature and pressure (Fig. 1). All reactions were conducted in the presence of 0.5 g/L of glucose aqueous solution, with a weight ratio Glucose/Catalyst of 1 and under **15 bar of argon** and the mixture was mechanically stirred at 500 rpm. Only temperature and irradiation varied: i) hydrothermal reactions were conducted at **120 or 150 °C** without irradiation, ii) photocatalytic reactions were conducted at ambient temperature and under UV irradiation (**PLL-lamp: 18 W, 365 nm and 6.2 mW cm^{-2}**) and iii) **hydrothermal reactions assisted by photocatalysis** were conducted at **120 or 150 °C** and under the same **UV irradiation** than photocatalytic reactions.

The reactions are started as follows: first water and TiO_2 are placed in the autoclave and brought to the reaction temperature, then the adequate glucose amount was introduced (solubilized in few mL of water) and UV irradiation started immediately if necessary, this is the zero time of the reaction.

In order to investigate the stability and recyclability of commercial TiO_2, the catalyst was separated from reactional medium by centrifugation and then washed by water and dried at 70 °C for 3 h. The dried catalyst was used in glucose hydrothermal transformation assisted by photocatalysis (120 °C and under UV irradiation).

Glucose conversion (%) and products yields (%C) are calculated as follows:

$$\text{Conversion (\%)} = (\text{Glucose consumed})/(\text{initial Glucose}) * 100$$

$$\text{Product i Yield (\%C)} = (\text{Product i molar concentration})/(\text{Glucose initial molar concentration}) * (\text{Product i carbon number})/6 * 100$$

2.3. Analytical procedures

2.3.1. High-Performance Liquid Chromatography (HPLC)

During the glucose transformation reactions, the glucose and the products in aqueous phase, were quantified by HPLC Shimadzu Prominence system equipped with a refractive index detector (RID), a photometric diode array detector (PDAD) and the products separation was done with a COREGEL 107 H column maintained at 40 °C. The mobile phase is acidified water (H_2SO_4 1.7 mM). The RID was used to detect the monosaccharides, the aldehydes and the ketones. While the PDAD was used to detect the carboxylic acids and furanic compounds at 210 nm (Fig. S1) [32]. Butyric acid was used as internal standard.

2.3.2. Gas chromatography with mass spectrometry detector (GC-MS)

The identification of some products was done by analyzing pure standards aqueous solutions diluted in acetonitrile (20:80 v/v) with GC-MS in particular to check the formation of levulinic acid (Fig. S2). A Shimadzu GC-2010 Plus equipped with a mass spectrometer detector (QP2010 SE), a capillary column (SLB-5 ms, L × I.D. 30 m × 0.25 mm, df 0.25 μ) and a splitless injection system was used. Injection temperature was 280 °C. The flow of carrier gas (helium) through the column was 1.8 mL/min and the head pressure on the column was maintained at 101 kPa. Temperature program was as follows: 40 °C hold for 5 min, 20 °C min^{-1} to 70 °C, hold for 5 min, 20 °C min^{-1} to 100 °C, hold for 5 min, 20 °C min^{-1} to 120 °C, hold for 10 min, 20 °C min^{-1} to 150 °C, hold for 10 min, of 20 °C min^{-1} to 200 °C, hold for 10 min. And mass spectrometer was set as follows: ion source temperature at 200 °C and voltage relative to the tuning result of 0.2 kV.

2.3.3. Total organic carbon

To determine the carbon balance in liquid phase at the end of the reaction, a Shimadzu TOC-VSCH total organic carbon (TOC) was used to quantify the total mass of carbon in the liquid phase (residual glucose and products). It consisted in the mineralization of the organic compounds at 720 °C catalyzed by Pt/Al_2O_3 into CO_2 that was then quantified by IR detector. The carbon balance was then calculated by dividing the TOC measured at the end of reaction (final TOC) by the initial TOC

Table 1
Main physico-chemical properties of commercial TiO_2: UV100 and Rut160 [32].

	UV100	Rut160[a]
Crystalline phase[b]	Anatase	Rutile
Crystallite size[b] (nm)	7.5	8.5
Glucose adsorption capacity[c] (μmol m^{-2})	0.7	0.3
Acid sites density[d] (μmol m^{-2})	3	1.37
Basic sites density[e] (μmol m^{-2})	0.4	0.23
Basic/Acid sites ratio	0.13	0.17
Specific surface area[f] (m^2 g^{-1})	300	175

[a] pretreatment: 2 h at 400 °C. [b] from XRD patterns. [c] aqueous phase, 30 °C. [d] calorimetry of NH_3 adsorption. [e] calorimetry of CO_2 adsorption, [f] Brunauer, Emmett and Teller (BET): pretreatment for 2 h at 300 °C (Temperature ramp: 5 °C mn^{-1}), N_2 adsorption.

[32].

C balance (%) = final TOC/initial TOC * 100

2.4. Gas phase analysis

Gas phase analysis was performed using a Clarus 590 gas phase chromatogram (Perkin Elmer). The gas products are first separated with a PoraPlot Q column (25 m × 0.53 mm × 20 μm df – Agilent J&W Technologies). The flow is then divided and directed in parallel to two detectors: on one side a Polyarc (R) system (Activated Research Company) (293 °C, air flow of 2.5 mL/min and H_2 flow of 35 mL/min) coupled to a flame ionization detector (FID), on the other side to an automated selection valve feeding an RT-Msieve5A molecular sieve type column (30 m × 0.32 mm × 30 μm df – Restek) and a pulsed discharge helium ionization detector (PDHID) (VICI). The lighter compounds (H_2, Ar, O_2, N_2, CH_4, CO) are sent over the molecular sieve, and the rest of the flow goes to the vent. The Polyarc system is formed by two successive catalytic beds to oxidize the organic analytes (C_2H_4…) to CO_2 before

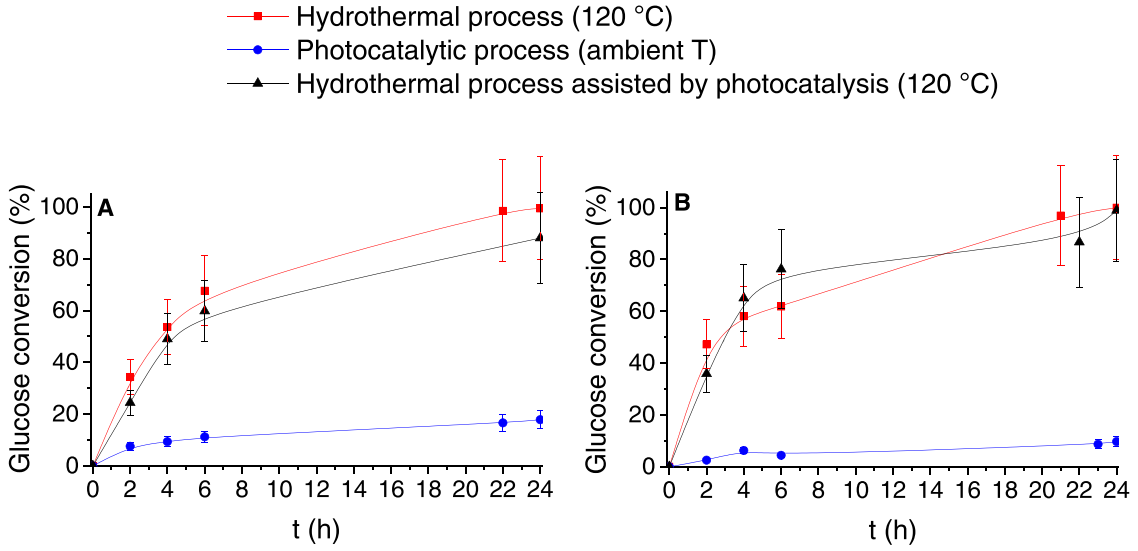

Fig. 2. Glucose conversion time course under hydrothermal conditions and/or photocatalytic conditions in presence of UV100 (A) and Rut160 (B). *Conditions: P = 15 bar of Ar, [glucose] = [TiO_2] = 0.5 g L^{-1}, T = 120 °C and UV free for hydrothermal process, ambient temperature and UV irradiation for photocatalytic process, 120 °C and UV irradiation for hydrothermal process assisted by photocatalysis.*

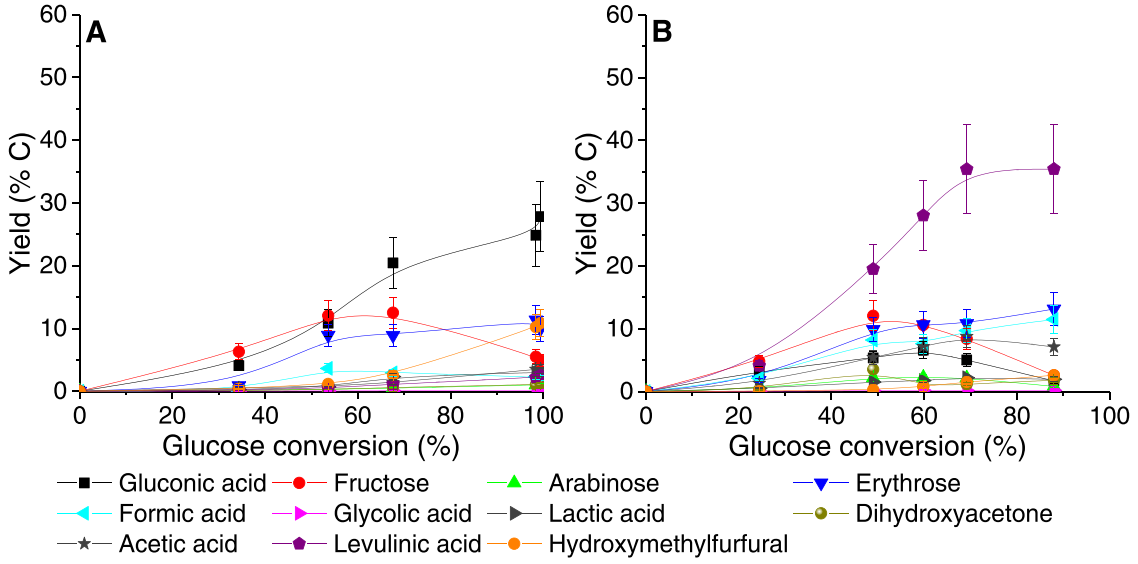

Fig. 3. Product's yield evolution with glucose conversion by hydrothermal process not assisted (A) and assisted (B) by photocatalysis in presence of UV100. *Conditions: P = 15 bar of Ar, [glucose] = [TiO_2]= 0.5 g L^{-1}, T = 120 °C, UV irradiation (no irradiation for hydrothermal process).*

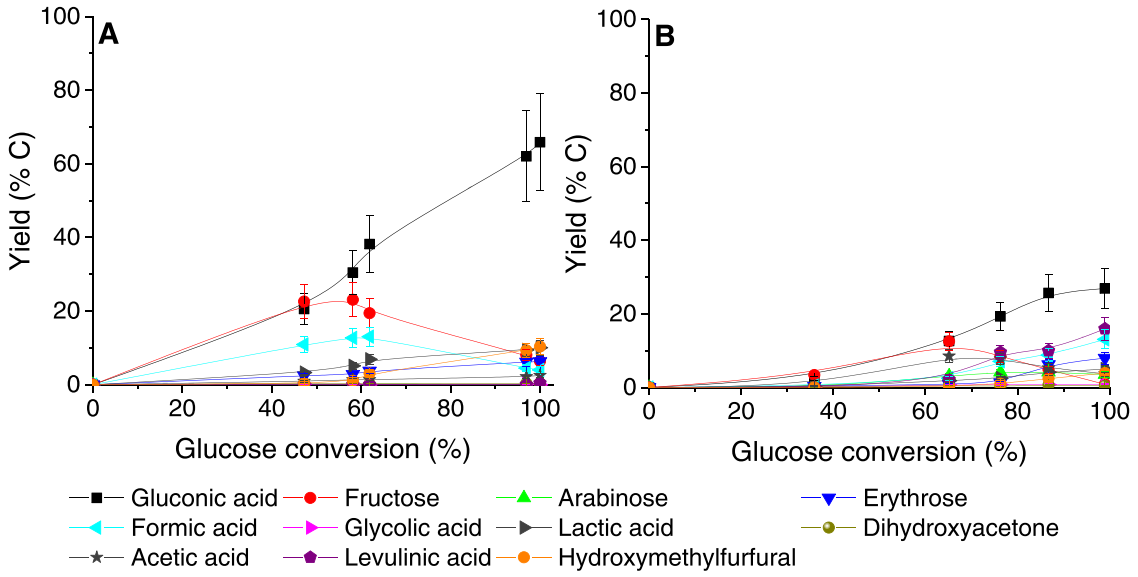

Fig. 4. Product's yield evolution with glucose conversion by hydrothermal process not assisted (A) and assisted (B) by photocatalysis in presence of Rut160. *Conditions: P = 15 bar of Ar, [glucose] = [TiO_2] = 0.5 g L^{-1}, T = 120 °C, UV irradiation (no irradiation for hydrothermal process).*

reducing them to CH_4 and detected by FID. The initial oven temperature was 50 °C, increasing by 20 °C min^{-1} to 150 °C after which the temperature was held until the end of analysis. The injection port temperature was 150 °C and FID and PDHID temperature were 250 °C. And for FID, air and H_2 flows were 450 and 10 mL min^{-1}, respectively.

3. Results and discussion

3.1. Physico-chemical properties of the commercial TiO_2

The physico-chemical properties of the commercial TiO_2, UV100 and Rut160, were investigated elsewhere [32]. They are recalled in Table 1.

To summarize, UV100 has a pure anatase phase and Rut160 only the rutile one. The BET surface area of UV100 is almost twice that of Rut160. The capacity of glucose adsorption in aqueous phase of UV100 is also twice that of Rut160 and was previously correlated to its higher Lewis acid sites density [32]. As regards to their acid-base properties, pyridine adsorption monitored by FTIR has detected only Lewis acid sites [32], besides NH_3 and CO_2 adsorption monitored by calorimetry has shown that Rut160 has a more basic surface than UV100 with basic/acid sites ratios equal to 0.17 and 0.13, respectively.

3.2. Comparison of combined processes to separated ones

3.2.1. Anatase (UV100) and rutile (Rut160) catalytic activity

The performance of hydrothermal process assisted by photocatalysis (120 °C) was compared to pure hydrothermal (120 °C) and pure photocatalytic (ambient T) processes for glucose transformation. The kinetic of glucose conversion by hydrothermal process assisted by photocatalysis at 120 °C, in presence of UV100 (anatase) (Fig. 2. A) and Rut160 (rutile) (Fig. 2. B), followed the same trend as the UV free hydrothermal process performed also at 120 °C, with very close initial rates of glucose disappearance and the complete glucose conversion after 24 h of reaction. This is more efficient than the photocatalytic process, performed at ambient temperature, with a glucose conversion below 20% and 10% after 24 h over UV100 and Rut160, respectively.

Even if the rate of glucose conversion was similar by the combined process and by the hydrothermal one, the nature of the major product and their evolution in liquid phase with glucose conversion were different as shown in Fig. 3 for UV100 or Fig. 4 for Rut160, but no new product was observed. The observed products were: fructose, arabinose, erythrose, dihydroxyacetone, 5-HMF and several carboxylic acids: gluconic, formic, glycolic, lactic, acetic and levulinic acids. In our previous work, the same products were observed from glucose transformation in the hydrothermal or photocatalytic processes performed under air in presence of UV100 and Rut160 [32]. Since the present studies are performed under Ar atmosphere, using degassed water, this first observation on the same nature of products formed from glucose under Ar or air atmosphere could suggest that molecular oxygen would not be the main source of oxygen for gluconic acid formation. Most likely, water could be the oxygen vector as previously demonstrated for aerobic 5-HMF oxidation into furan dicarboxylic acid (FDCA) using $H_2{}^{18}O$ over TiO_2 supported Au catalyst [33]. This would proceed via a simple hydration of the aldehyde group of glucose catalyzed by the superficial basic sites of TiO_2 (Scheme 1).

Even if UV100 was almost inactive under photocatalytic conditions, at ambient T, because of electron-holes pairs' recombination under inert atmosphere (Ar) (Fig. S3 in Supplementary information), assisting hydrothermal process at 120 °C by photocatalysis changed radically the nature of the major product from gluconic acid to levulinic acid (Fig. 3). Indeed, under anaerobic condition at 120 °C, under UV free conditions, 30% yield of gluconic acid was achieved after 24 h with the

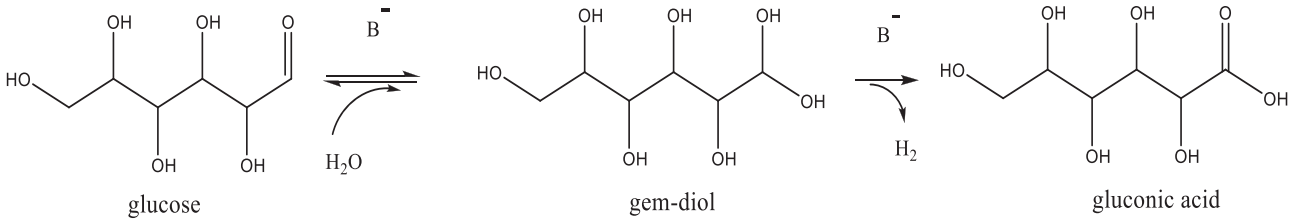

Scheme 1. Proposed base catalyzed hydration of the C1 aldehyde group of glucose into gem-diol and its further dehydrogenation into gluconic acid.

Table 2
Liquid carbon balance (from TOC analysis) after 24 h.

Catalyst	Carbon balance after 24 h (%)		
	Hydrothermal process	Photocatalytic process	Hydrothermal process assisted by photocatalysis
UV100	96 ± 5	91 ± 5	78 ± 4
Rut160	100 ± 5	100 ± 5	96 ± 5

Conditions: P = 15 bar of Ar, [glucose] = [TiO_2] = 0.5 g L^{-1}, T = 120 °C and UV free for hydrothermal process, ambient temperature and UV irradiation for photocatalytic process, 120 °C and UV irradiation for hydrothermal process assisted by photocatalysis.

intermediate formation of fructose up to a maximum yield of 12%. Upon UV irradiation at 120 °C, levulinic acid becomes the main product, with a yield of 35% observed after 24 h while the gluconic acid became a minor product after 24 h, at nearly full glucose conversion in both processes. Besides, fructose presents a maximum yield of 12% at half glucose conversion up to its complete disappearance with the reaction progress. Note that it is well known that equilibrium glucose-fructose is a base or Lewis acid catalyzed step, and both type of sites exist on UV100 and Rut160 TiO_2. Thus, the evolution of the fructose yield with the course of the reaction could indicate the behavior of an intermediate product but could be simply due to the glucose depletion with time. Moreover, formic and acetic acids were more produced with the combined process and 5-HMF was less produced, in agreement with its likely transformation into levulinic acid. With the hydrothermal process, only 2.5% yield of formic acid and 2.2% yield of acetic acid were obtained at conversion of 80%, while at this conversion level with the hydrothermal process assisted by photocatalysis, 11% of formic acid and 8% of acetic acid were obtained. Let us recall that formic acid is co-produced with levulinic acid in the Brønsted acid catalyzed hexoses conversion in levulinic acid [3].

Carbon balance in presence of UV100 at 24 h, at full glucose transformation, was around 95% with the UV free hydrothermal process and 80% with the combined process (Table 2). This difference can be explained by products formation in gas phase in higher quantities by the combined process than the UV free hydrothermal one (Fig. 5). CO_2, CO and H_2 were observed with both processes (Fig. 5). Interestingly, ethylene which is a very interesting platform molecule was produced only by the combined process in presence of UV100: 32 μmol (Fig. 5).

By contrast to UV100, assisting glucose hydrothermal treatment by photocatalysis didn't change the nature of the main products in presence of Rut160 (Fig. 4). However, the products distribution and their total amounts detected by HPLC changed upon UV irradiation. A very high gluconic acid yield of 70% was achieved at complete glucose conversion with the UV free hydrothermal process. Such a high yield was unexpected because gluconic acid is a direct glucose oxidative product and the hydrothermal process was conducted under Ar, air being flushed several times before starting the reaction and water being degassed. Gluconic acid yield reached a maximum yield of 7% at 70% glucose conversion under air (5 bar) (Fig. S4 in Supplementary information) in equivalent temperature conditions, while it reached 45% under Ar at the same glucose conversion of 70% (Fig. 4). This can be explained by its further oxidation under air. Moreover, Rut160 produced much more gluconic acid than UV100: at 100% glucose conversion, the gluconic acid yields were respectively 70% and 30%. In our previous work [32], we investigated in details the acid base properties of UV100 and Rut160. Rut160 has a more basic surface than UV100 [32]. More precisely, its Lewis basic/acid sites balance is higher (Table 1). Accordingly, it seems reasonable to propose that in anaerobic and hydrothermal conditions, the superficial basic sites (O^{2-}) of Rut160, interacting with water, would provide active basic hydroxyl groups which would be very efficient for gluconic acid formation, in other word to promote base catalyzed

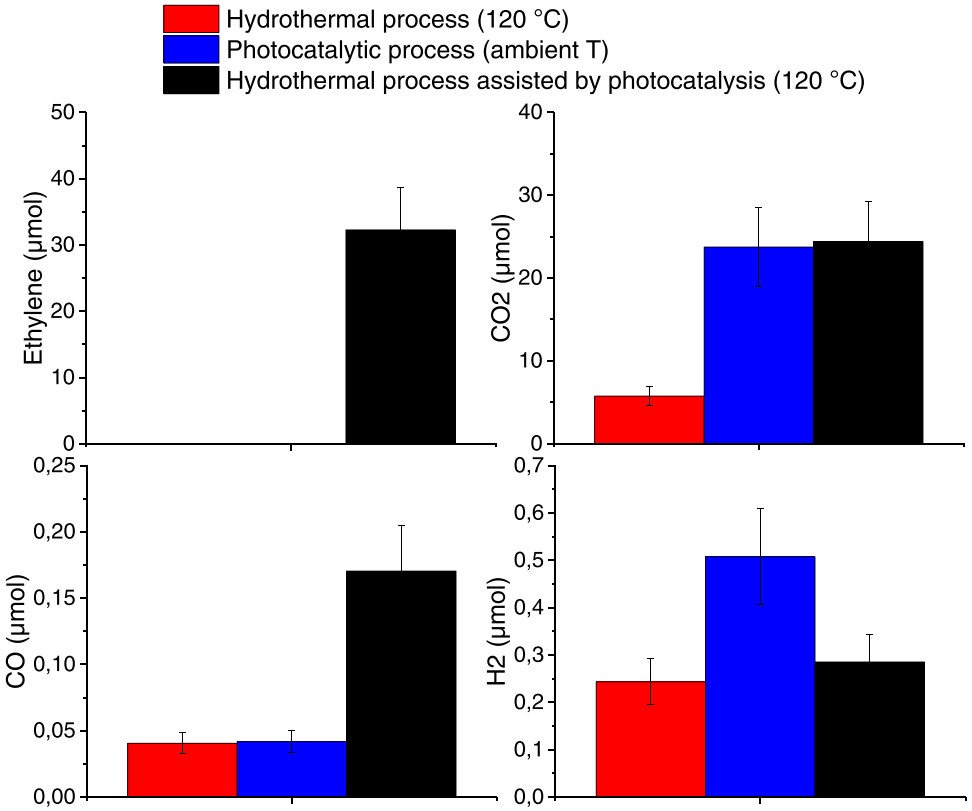

Fig. 5. Gas phase composition after 24 h under hydrothermal and/or photocatalytic conditions with UV100 under 15 bar of Ar. *Conditions: P = 15 bar of Ar, [glucose] = [TiO_2] = 0.5 g L^{-1}, T = 120 °C and UV free for hydrothermal process, ambient temperature and UV irradiation for photocatalytic process, 120 °C and UV irradiation for hydrothermal process assisted by photocatalysis.*

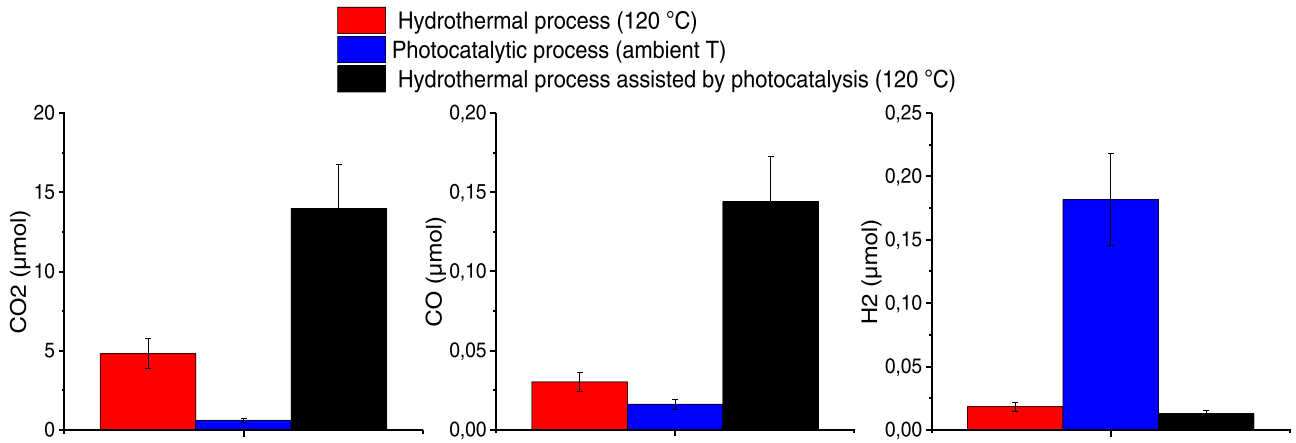

Fig. 6. Gas phase composition after 24 h under hydrothermal and/or photocatalytic conditions with Rut160 under 15 bar of Ar. *Conditions: P = 15 bar of Ar, [glucose] = [TiO$_2$] = 0.5 g L^{-1}, T = 120 °C and UV free for hydrothermal process, ambient temperature and UV irradiation for photocatalytic process, 120 °C and UV irradiation for hydrothermal process assisted by photocatalysis.*

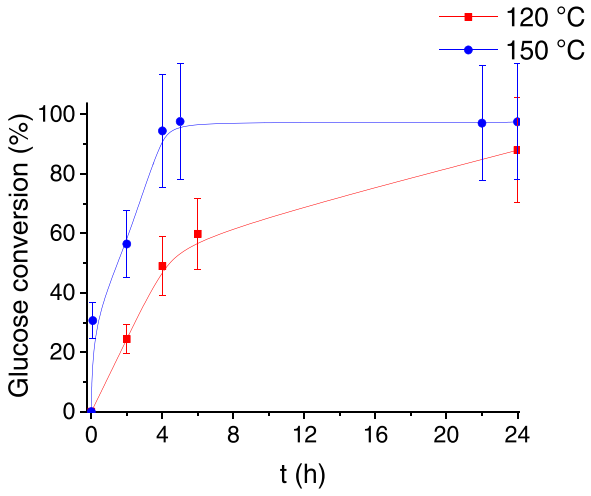

Fig. 7. Temperature effect on glucose conversion time course by hydrothermal process (120 °C and 150 °C) assisted by photocatalysis in presence of UV100. *Conditions: P = 15 bar of Ar, [glucose] = [TiO$_2$] = 0.5 g L^{-1}, T = 120 or 150 °C, UV irradiation.*

hydration of the C1-aldehyde group of glucose into a gem-diol and then into gluconic acid as shown in Scheme 1. This proposition is well supported by the role of water disclosed by Davis et al. in the aerobic aldehyde group oxidation of 5-HMF to get FDCA [33]. One can underline that the gluconic acid yield, around 70%, is of the same order of magnitude than those obtained with supported noble metals (Pt, Pd) used in presence of soluble bases [34] or in base free conditions for Au containing bimetallic catalysts [35,36]. As regards to the previous metallic catalytic systems, the use of a basic TiO_2 such as Rut160 presents as main advantage to be a noble metal free catalyst, avoiding the use of homogeneous bases and in addition which overcomes the noble metal leaching problems, the main drawbacks of metallic catalysts used in oxidation reactions in hydrothermal conditions.

Upon UV irradiation, at full glucose conversion, the gluconic acid yield was reduced by a half while the levulinic and formic acid yields increased significantly. The products evolution follows the same tendency to that observed over UV100 upon UV irradiation but the extent of the changes is limited: at the reaction end, gluconic acid remains the major product with a yield reduced from 70% without UV down to 30% with UV and the levulinic acid yield achieved ~ 15% after 24 h. Moreover, over Rut160, one can observe that the sum of the products' yields detected by HPLC was reduced upon UV irradiation by comparison to the UV free conditions. This can be explained by more soluble oligomers' formation (not detected by HPLC) by the combined process compared to the hydrothermal one. Indeed, the carbon balance determined by the total organic carbon (TOC) measurement at the end of the reaction was close to 100% (Table 2) for Rut160 with those two processes.

In gas phase, hydrogen, carbon dioxide and monoxide were detected under hydrothermal and/or photocatalytic conditions in presence of Rut160 (Fig. 6). But ethylene was not observed with combined processes unlike UV100.

3.2.2. Temperature effect

Glucose transformation was also studied at 150 °C to determine the temperature effect combined with UV irradiation on selectivity in presence of the most selective catalyst in levulinic acid and ethylene: UV100. As at 120 °C, the kinetic of glucose conversion by hydrothermal process at 150 °C assisted by photocatalysis was almost the same than by hydrothermal process (Fig. S6 in Supplementary information). Besides, glucose conversion was initially more rapid at 150 °C than at 120 °C and reached 100% after 5 h of reaction at 150 °C while more than 6 h are required at 120 °C (Fig. 7).

Similarly, the UV irradiation doesn't change the nature of the products at 150 °C but it changed their distribution, their evolutions and their total amounts (Fig. 8):

i) The major product changed from gluconic acid in absence of UV irradiation to levulinic acid under UV irradiation.
ii) Again, formic and acetic acids were more produced with the combined process. For hydrothermal process, 3% of formic acid and 2% of acetic acid were obtained at high conversion, 90%. While at this conversion level, with the hydrothermal process assisted by photocatalysis, 14% of formic acid and 6% of acetic acid are obtained.
iii) 5-HMF was less produced when hydrothermal process was assisted by photocatalysis most likely due to its transformation into levulinic acid obtained at the maximized yield of 60% at glucose conversion of 95%.

When the reaction was prolonged reaching the complete glucose conversion after 24 h for the combined process, the levulinic acid yield decreased drastically to 0.1% (Fig. 8) and ethylene and hydrogen were much more produced at 150 °C than at 120 °C (Fig. 9). Three times more ethylene was produced by increasing the temperature from 120 °C to 150 °C, 32 versus 94 µmol respectively. Hydrogen was produced in significant amount at 150 °C, with a total amount of 180 µmol at 150 °C

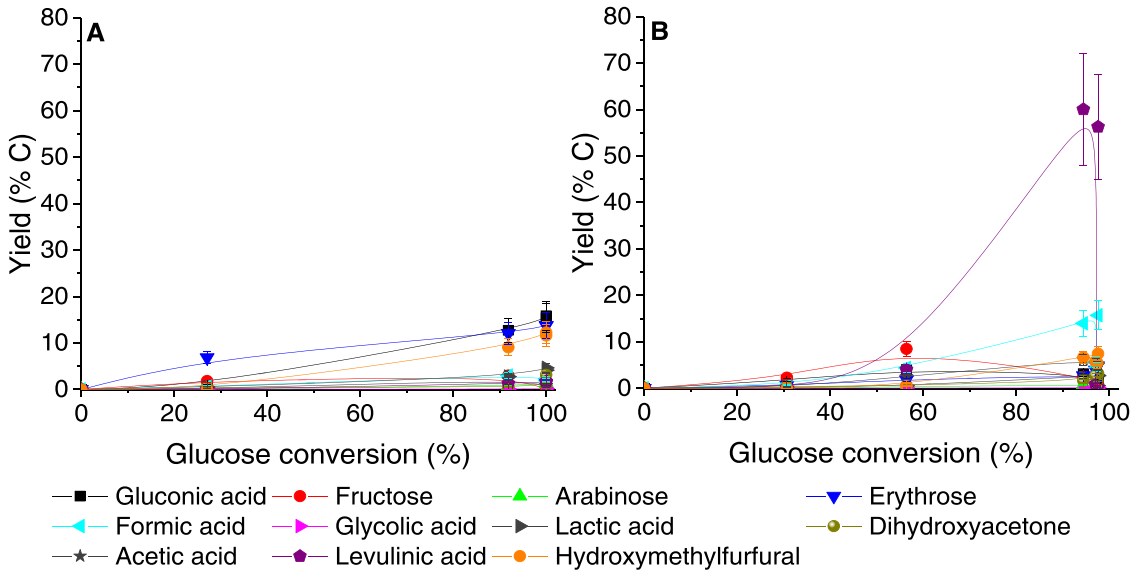

Fig. 8. Product's yield evolution with glucose conversion by hydrothermal process not assisted (A) and assisted (B) by photocatalysis in presence of UV100 at 150 °C. *Conditions: P = 15 bar of Ar, [glucose] = [TiO_2] = 0.5 g L^{-1}, T = 150 °C, UV irradiation (no irradiation for hydrothermal process).*

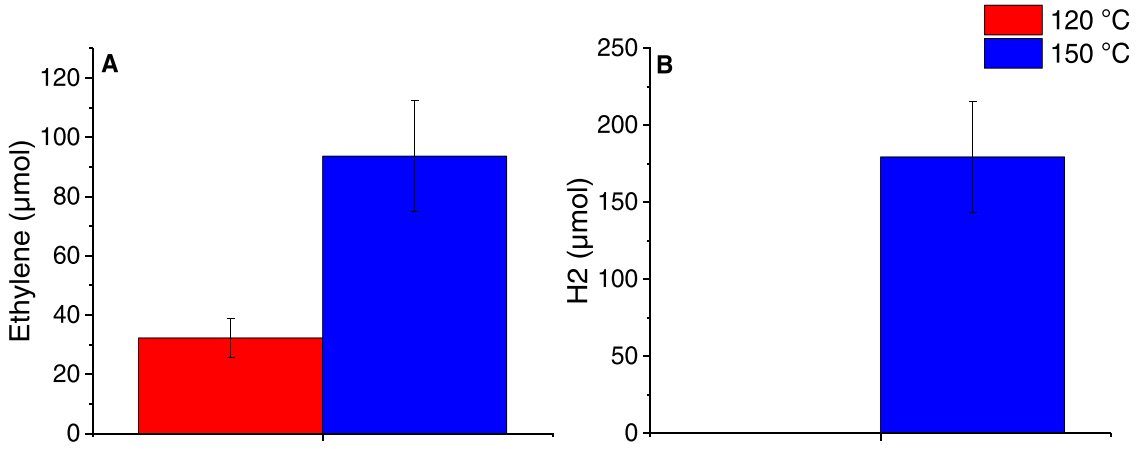

Fig. 9. Temperature effect on ethylene (A) and H_2 (B) production by hydrothermal process assisted by photocatalysis in presence of UV100. *Conditions: P = 15 bar of Ar, [glucose] = [TiO_2] = 0.5 g L^{-1}, T = 120 or 150 °C, UV irradiation.*

against 0.28 µmol at 120 °C. It appears that glucose transformation by hydrothermal process assisted by photocatalysis can be conducted selectively to produce levulinic acid when it is stopped at 95% of conversion or to hydrogen and ethylene when it is prolonged at complete glucose conversion.

Note that for the UV free hydrothermal process, the temperature' increase from 120 to 150 °C didn't favor the levulinic acid production with a yield lower than 4% (Fig. S7 in Supplementary information) by contrast to the hydrothermal process assisted by photocatalysis where rising the temperature from 120 to 150 °C increased the maximum levulinic acid yield from a plateau at 35–60% at ~ 90% conversion (Fig. 10).

An important general remark can be drawn from the data displayed in Figs. 3 and 8: assisting glucose hydrothermal process by UV irradiation at high temperature, 150 °C, is disclosed as an efficient way to improve the selectivity of the hydrothermal process in value added molecules. This combined process overcomes the main drawback of the hydrothermal ways for carbohydrates valorization: the inescapable carbon losses as polymers formation (humins) which makes this process non-selective.

The nature of the favored product upon UV irradiation at 150 °C, levulinic acid, a product usually obtained via strong mineral acid catalyzed hexoses transformation, raises many questions because the original TiO_2 surface has not the required strong Brønsted acidity. Let us recall here that we have previously shown by pyridine adsorption followed by FTIR that both TiO_2, UV100 and Rut160, present only Lewis acid sites, at least, after dehydration at relatively low temperature, 150 °C [32].

Thus, our catalytic data strongly suggest that the UV irradiation could be at the origin of a strengthening of the Brønsted acidity of the reaction medium. The question is: what is (are) the phenomenon(a) at the origin of the acidity enhancement?

A first explanation could be related to the many carboxylic acids formed in the reaction medium via the previously assumed base catalyzed glucose and other derived aldoses (arabinose, erythrose) hydration. This could provide the required homogeneous Brønsted acidity. However, few articles reported that levulinic acid could be obtained from hexose using homogenous carboxylic acids [37]. Otherwise, in presence of carboxylic acid aqueous solutions whatever be the nature or its concentration, De Souza et al. obtained effectively 5-HMF from fructose [7] and they observed that those acids can hardly catalyze the successive step of 5-HMF rehydration in levulinic and formic acid. The

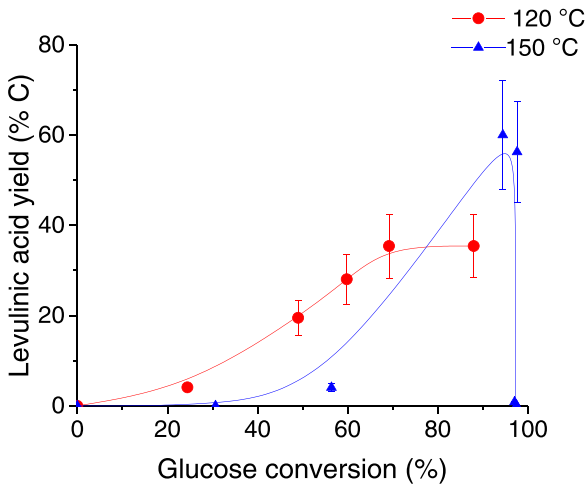

Fig. 10. Temperature effect on levulinic acid yield evolution with the glucose conversion by hydrothermal process assisted by photocatalysis in presence of UV100. *Conditions: P = 15 bar of Ar, [glucose] = [TiO$_2$] = 0.5 g L^{-1}, T = 120 or 150 °C, UV irradiation.*

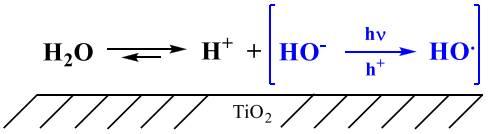

Scheme 2. Assumed impact of the UV irradiation on a possible right shifting of water self protolysis equilibrium on the first few layers of hydration of TiO_2 with a possible Brønsted acid sites creation on the hydrated TiO_2 surface.

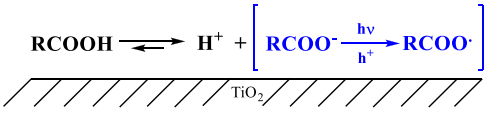

Scheme 3. Proposed impact of the UV irradiation on a possible right shifting of carboxylic acid dissociation equilibrium on the TiO_2 surface with a possible Brønsted acid sites creation on the TiO_2 surface.

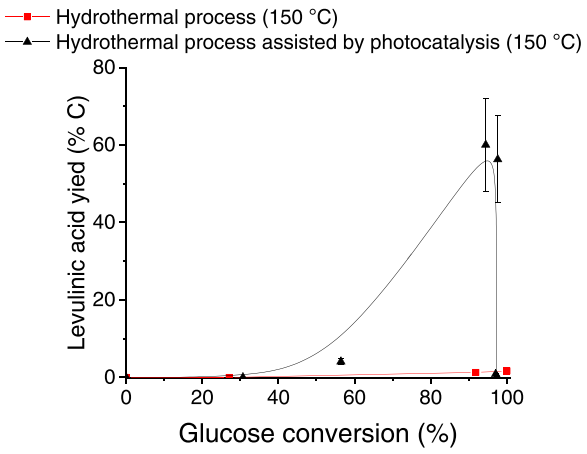

Fig. 12. Comparison of levulinic acid production by the hydrothermal process assisted or not by photocatalysis in presence of UV100 at 150 °C. *Conditions: P = 15 bar of Ar, [glucose] = [TiO$_2$] = 0.5 g L^{-1}, T = 150 °C and UV irradiation for hydrothermal process assisted by photocatalysis, UV free and 150 °C for hydrothermal process.*

former products are generally obtained using stronger acid solutions based on H_2SO_4 as previously recalled.

Another explanation could rely on the direct consequence of the UV irradiation on the TiO_2 surface, producing electron-hole pairs and their possible impact on water self protolysis occurring in the first hydration layers of the irradiated TiO_2 surface. This could result in a right shifting of water self protolysis equilibrium via hydroxyl groups neutralization by the hole (h^+) as previously reported [38]. This situation could simply provide the strong Brønsted acidity required on the TiO_2 surface which, combined with the thermal activation brought by the high temperature, could explain the formation of levulinic acid from glucose upon UV irradiation (Scheme 2).

Following the same idea, we cannot exclude that the first carboxylic acids formed in the reaction media could also be "neutralized" by the holes, h^+, created upon TiO_2 UV irradiation and provide on the TiO_2 surface a relative "free" proton capable to promote levulinic acid formation (Scheme 3).

In order to consolidate or not these assumptions and to understand more the origin of the levulinic acid formation upon UV irradiation, the

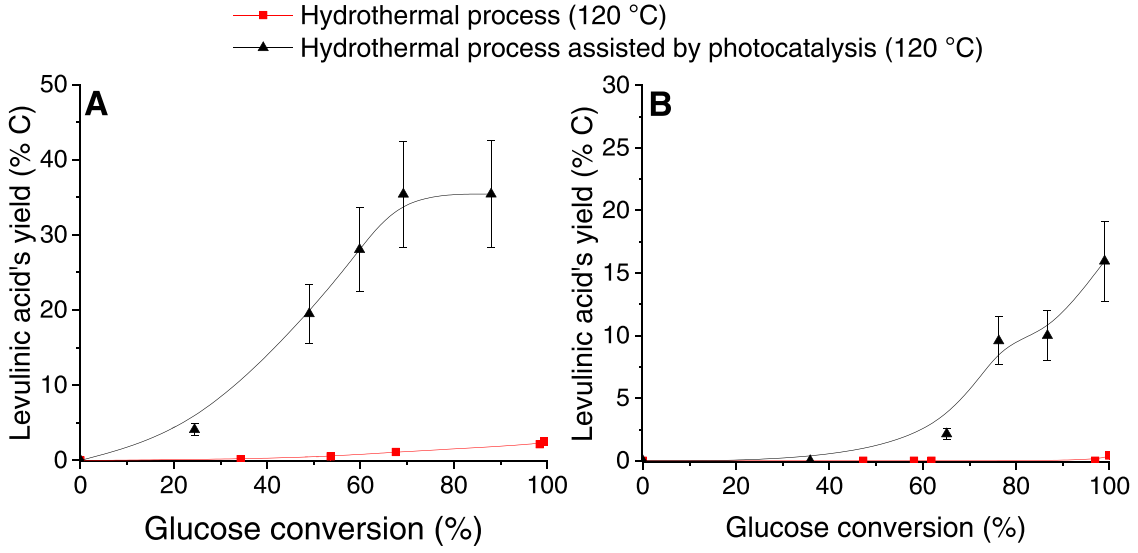

Fig. 11. Comparison of levulinic acid production by the hydrothermal process assisted or not by photocatalysis in presence of: UV100 (A) and Rut160 (B) at 120 °C. *Conditions: P = 15 bar of Ar, [glucose] = [TiO$_2$] = 0.5 g L^{-1}, T = 120 °C and UV irradiation for hydrothermal process assisted by photocatalysis, UV free and 120 °C for hydrothermal process.*

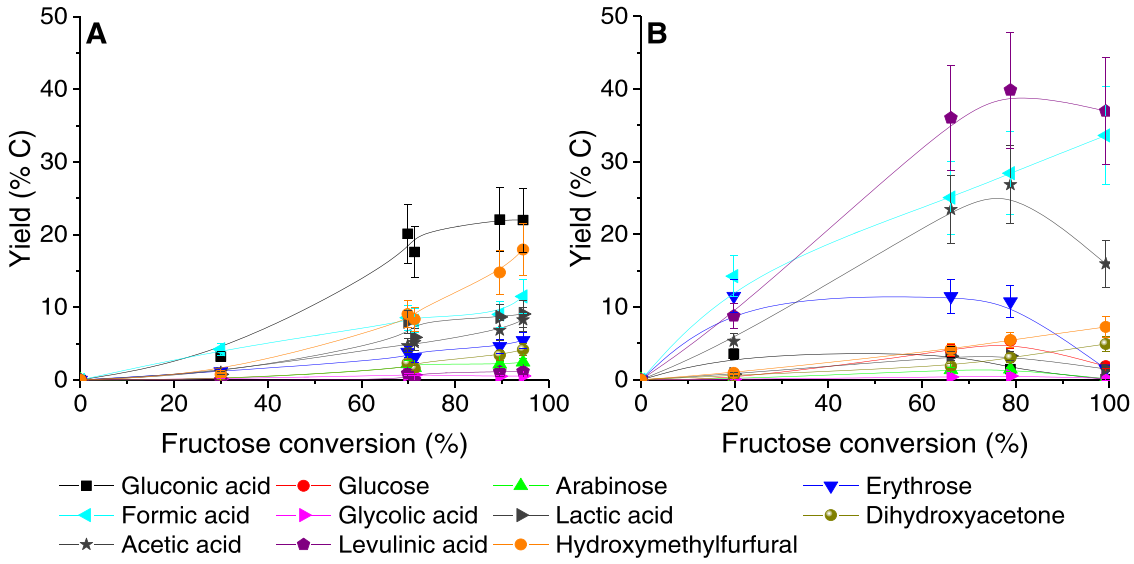

Fig. 13. Product's yield evolution with fructose conversion by hydrothermal process not assisted (A) and assisted (B) by photocatalysis in presence of UV100. *Conditions: P = 15 bar of Ar, [fructose] = [TiO_2]= 0.5 g L^{-1}, T = 120 °C and UV irradiation for hydrothermal process assisted by photocatalysis, UV free and 120 °C for hydrothermal process.*

reactivity of various possible intermediates under UV irradiation at high temperature was studied.

3.2.3. *Attempts to understand the origins of levulinic acid formation*

Levulinic acid formation was remarkably enhanced by assisting glucose hydrothermal treatment by photocatalysis with both anatase (UV100) and rutile (Rut160) catalysts as shown in Fig. 11 at 120 °C and in Fig. 12 at 150 °C. At equivalent conversion level of 70%, UV100 produced more levulinic acid (35%) than Rut160 (5%) at 120 °C (Fig. 11) and a maximum yield of levulinic acid of ~ 60% is reached at 150 °C over UV100 (Fig. 12).

It was generally accepted in the literature that levulinic acid is formed by hydration of 5-HMF, obtained by dehydration of fructose (glucose isomer), efficiently catalyzed by strong Brønsted acids such as H_2SO_4 or HCl [3,5,39].

To understand more the levulinic acid formation pathway, we studied the conversion of fructose in presence of the most efficient catalyst for levulinic acid formation: UV100. First, the coupling effect was verified. Fructose conversion by hydrothermal process assisted by photocatalysis was compared to the two separated processes, UV free hydrothermal one at 120 °C and the photocatalytic one at ambient temperature. The three processes led to an initial fast fructose consumption even the photocatalytic one performed at ambient temperature. The fructose conversion reached a plateau at a conversion level of 60% after 2 h with the pure photocatalytic process at ambient temperature while the two other processes at 120 °C led to the complete fructose conversion after 24 h (Fig. S8 in Supplementary information). As for glucose, assisting hydrothermal process by photocatalysis changed the nature of the major products from gluconic acid and 5-HMF to levulinic acid, and formic acids under the combined process (Fig. 13). Note that, under UV free conditions, more 5-HMF are obtained from fructose, in agreement with its higher reactivity than glucose. However, equivalent levulinic acid yields were obtained in the hydride process whatever be the hexose (Fig. 13 versus Fig. 3). We have also studied the conversion of 5-HMF by hydrothermal process assisted by photocatalysis in presence of UV100, without and with addition of formic/acetic acids, in amount equivalent to their maximum concentration obtained by glucose transformation by the hybrid process. Interestingly, it is shown that 5-HMF is hardly converted within the hybrid process leading to a low yield of Levulinic acid with or without addition of formic/acetic acid in the reaction media (Fig. S11 in Supplementary information). The different behaviors between the hexoses and 5-HMF for levulinic acid formation when hydrothermal conditions are combined to the UV irradiation might originated in distinct adsorption capacities which probably is a prerequisite to take advantages of the electronic modification of the TiO_2 surface upon irradiation via a favored substrate adsorption on its surface. Accordingly, UV100 was previously shown to adsorb more glucose than Rut160 (Table 1).

Finally, to get a better understanding of the irradiation effect on levulinic acid production, we studied glucose conversion by hydrothermal process assisted by photocatalysis by irradiating the reactor only 4 h after reaction zero time. The kinetic of glucose conversion was almost the same under hydrothermal conditions without irradiation and with irradiation at 4 h (Fig. S12 in Supplementary information). First, one can underline that UV irradiation not only inhibits gluconic acid formation, but the amount of gluconic acid formed during the first 4 h are decomposed (Fig. 14.A) while levulinic acid yield increased remarkably (Fig. 14.D). Some other products observed in aqueous phase changed also upon UV irradiation i) fructose yield also decreased in a more pronounced way (Fig. 14.B), ii) 5-HMF yield increased but much less than without irradiation (Fig. 14.C) most likely because of its faster transformation into levulinic acid under UV irradiation than under UV free hydrothermal conditions and iii) the sum of formic and acetic acids yields increased remarkably after irradiation (Fig. 14.E).

In commercial processes such as the Biofine process, strong mineral acids such as sulfuric acid are used to produce levulinic acid at high temperature, around 200 °C, from the C6 sugars of lignocellulosic biomass under 14 bar. The byproducts are furfural and formic acid [3, 40]. Levulinic acid yield close to the theoretical one is obtained, ~ 50 wt % together with 20 wt% yield of formic acid based on hexoses. Levulinic acid production from glucose [5,9,39,41–44], fructose [9] or 5-hydroxymethylfurfural [41,42] has been also studied in presence of different types of catalysts (heterogeneous [5,9,42–44] or homogeneous [9,26,27] Brønsted acid catalysts) under hydrothermal conditions. It was observed that levulinic acid was generally produced in low yields at mild temperature and its yield increased at high temperature (> 170 °C). In fact, Ramli et al. observed only a levulinic acid yield of 13% at a conversion of 40% at 120 °C in presence of Fe/HY, a heterogeneous catalyst with Lewis and Brønsted acid sites and they achieved higher glucose conversion (100%) and levulinic acid yield of 55% when temperature was increased to 180 °C [42,43]. Thanks to UV irradiation, we succeeded to produce yields more than 35% of levulinic acid under

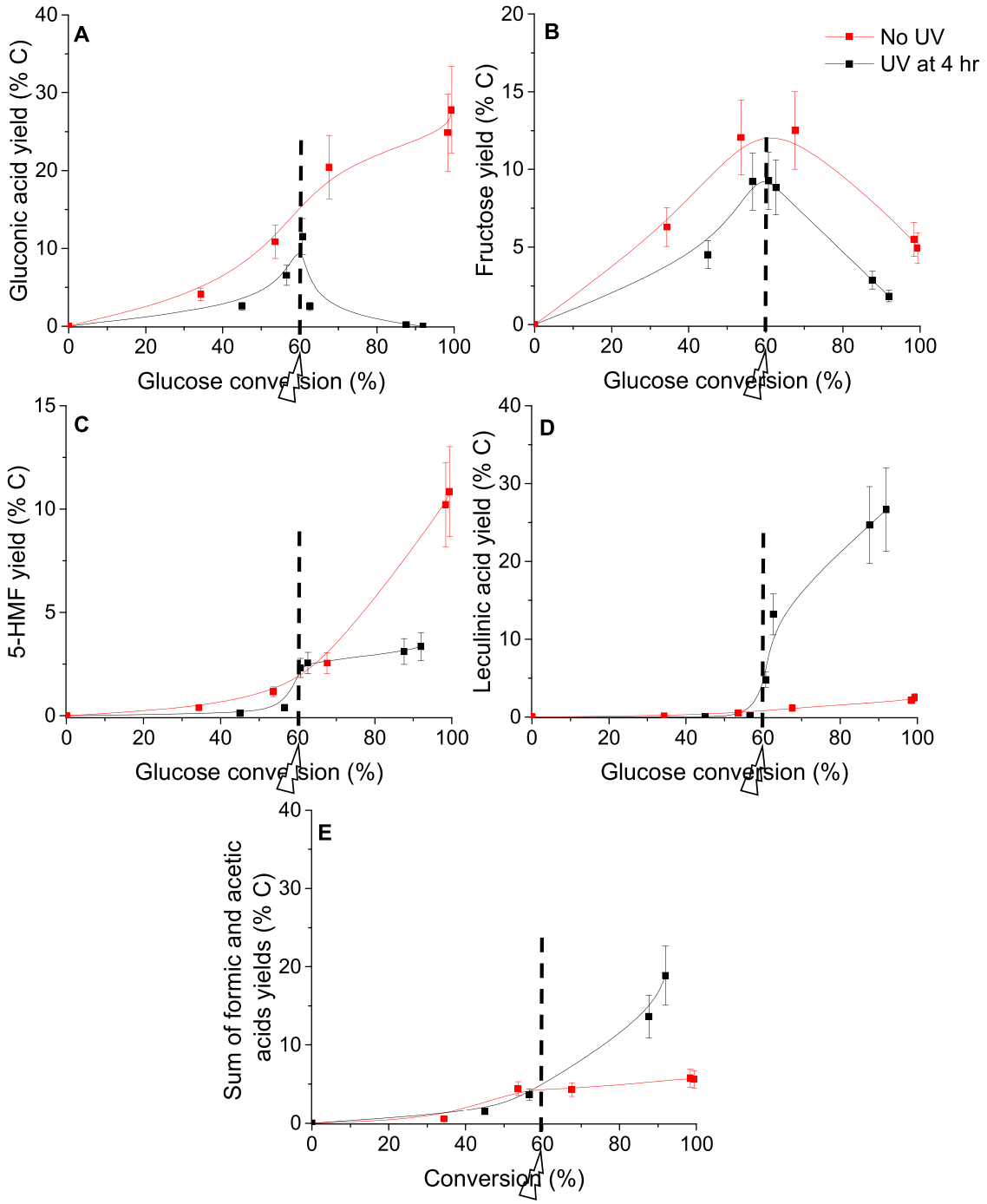

Fig. 14. Comparison of gluconic acid (A), fructose (B), 5-HMF (C), levulinic acid (D) and sum of formic and acetic acids (E) yield evolution with glucose conversion by hydrothermal process without irradiation (red) and with irradiation at 4 h (black). *Conditions: P = 15 bar of Ar, [glucose] = [TiO_2] = 0.5 g L^{-1}, T = 120 °C, UV irradiation.*

mild temperature, 120 °C, and ~ 60% at 150 °C with the heterogeneous TiO_2 catalyst having only Lewis acid sites and basic sites (UV100). While without irradiation, levulinic acid yield was lower than 10% at 120 °C with UV100. Thus, this innovative process, hydrothermal process assisted by photocatalysis, can give higher levulinic acid yield than usual hydrothermal treatment performed in presence of heterogeneous Brønsted acid catalysts avoiding the use of strong mineral acid such as H_2SO_4. These data provide indirect evidences that the UV irradiation in the presence of UV100 at 120–150 °C would make the TiO_2 suspension in aqueous media much more acidic than without UV irradiation. Possible explanations are given above with the participation of the surficial holes, h^+, created upon irradiation on the TiO_2 surface. However, at this stage we do not have direct proofs of the Brønsted acidity enhancement upon UV irradiation.

3.2.4. *Catalyst reusability*

The reusability and stability of catalyst is important for hydrothermal applications. For this purpose, the repeatability of UV100 in the hydrothermal transformation of glucose into levulinic acid assisted by photocatalysis was examined. As shown in Fig. 15, glucose conversion and levulinic acid yield were almost the same after 24 h even if some organic compounds are deposited on recovered catalyst surface (νC-H

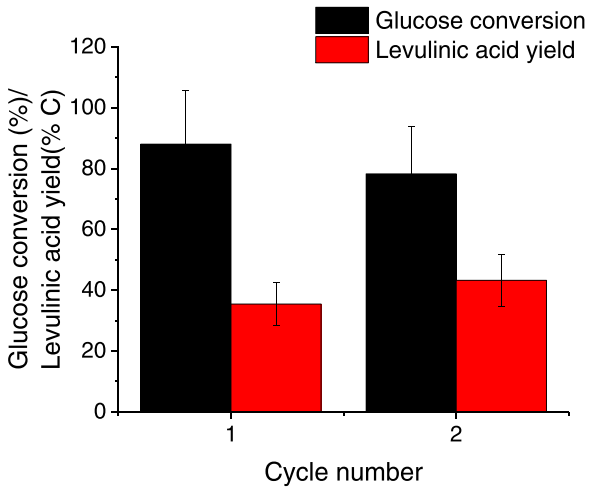

Fig. 15. Reusability of UV100 for hydrothermal transformation of glucose assisted by photocatalysis. *Conditions: P = 15 bar of Ar, [glucose] = [UV100] = 0.5 g L^{-1}, T = 120 °C, UV irradiation.*

characteristic vibrations between 3000 and 2800 cm^{-1} in Fig. S13 in Supplementary information). So, UV100 seems to be stable under hydrothermal conditions and reusable. Of course, several reuse cycles would have been necessary to determine its real stability.

3.3. Proposed overall pathway of glucose transformation by hydrothermal process assisted by photocatalysis

In the following, we have tried to rationalize the observed products distribution and their evolutions with or without UV, suggesting different reaction pathways which would be favored based on the conditions of irradiation and the nature of TiO_2.

From the products yields evolution in presence of UV100 (anatase) (Fig. 3), one can see that assisting hydrothermal process under Ar atmosphere by photocatalysis inhibited gluconic acid (Fig. 14.A) and its derivatives formation and highly favored levulinic acid formation. This drastic change could be explained by a change in catalyst's surface properties due to a change in electronic properties. In particular the formation of holes (h^+) in the TiO_2 at high temperature and under UV irradiation, is proposed to be the driving force for the formation of "free" protons, from water (Scheme 2) and/or from carboxylic acids (Scheme 3) whose acid strength would be high enough to promote levulinic acid formation from hexoses (pathway 2 in Scheme 4) at the expense of the base catalyzed gluconic acid formation and other C5, C4 sugars (pathway1 in Scheme 4).

The formation of ethylene could be initiated by the retro-aldolisation of fructose into erythrose and glycol aldehyde. The former one, once converted into dihydroxyacetone via a base catalyzed isomerization

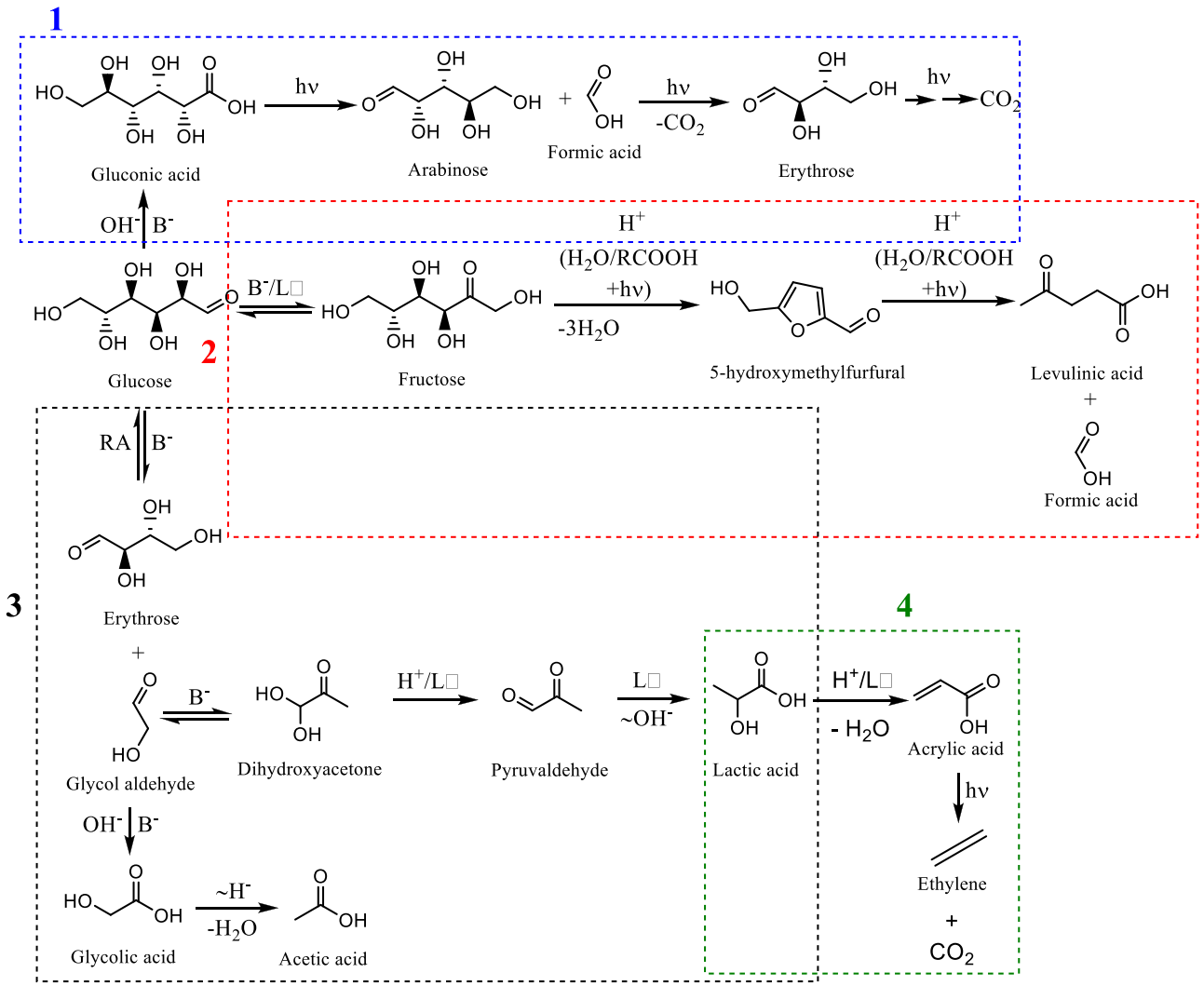

Scheme 4. Proposed glucose transformation pathways by hydrothermal process assisted by photocatalysis in presence of TiO_2.

could be further converted into lactic acid by Lewis acid sites (pathway 3 in Scheme 4). Lactic acid could be then dehydrated by Lewis acid sites and/or Brønsted acids into acrylic acid [45–48] which could be decarboxylated into ethylene under irradiation [22,49] (pathway 4 in Scheme 4).

The different behavior between UV100 and Rut160 could be explained considering their acid-base properties as follows:

1) The higher base/acid sites balance of Rut160 could explain its better catalytic performance for gluconic acid formation in UV free condition.
2) The higher density of Lewis acid sites of UV100, previously correlated to its higher capacity for glucose adsorption over Rut160 would explain its improved reactivity under UV irradiation, providing an optimum proximity between glucose adsorbed species and in situ generated H^+ at the TiO_2 surface and its higher levulinic acid production.

4. Conclusion

To conclude, assisting hydrothermal transformation of glucose by photocatalysis under mild temperature (120–150 °C) increased value added molecules yields and makes the hydrothermal process more selective minimizing its main drawback: the carbon losses in undesirable humins formation.

Levulinic acid production in liquid phase increased upon UV irradiation, especially in presence of TiO_2-UV100, at the expense of gluconic acid, with a parallel ethylene and hydrogen production in gas phase, especially at 150 °C.

Since levulinic acid is a molecule which require a strong Brønsted acidity to be formed from hexoses, our data could suggest that the reaction media is becoming more acidic upon irradiation. Indeed, the used titanium dioxide catalysts didn't have intrinsic Brønsted acid sites in reaction conditions; it is suggested that either the electronic changes of the TiO_2 under UV or the formation of carboxylic acids even if they're weak acids could be at the origin of the formation of levulinic acid. Other types of investigations such as theoretical studies or the direct in-situ demonstration of water protolysis are essential to confirm or not the hypothesis.

Finally, it is shown that in anaerobic condition, Rut160 'TiO_2 with a relative higher basic surface than UV100', is able to form selectively gluconic acid from glucose with a high yield of ~ 70%. This is of high interest since this result is obtained without soluble bases addition and with a noble metal free TiO_2 precluding the inescapable noble metal leaching in hydrothermal conditions.

CRediT authorship contribution statement

Insaf Abdouli: Investigation, Validation, Writing – original draft. **Frederic Dappozze:** Methodology, Formal analysis. **Marion Eternot:** Methodology, Formal analysis. **Nadine Essayem:** Funding acquisition, Supervision, Validation, Writing – review & editing. **Chantal Guillard:** Funding acquisition, Supervision, Validation, Writing – review & editing.

Declaration of Competing Interest

The authors declare that they have no known competing financial interests or personal relationships that could have appeared to influence the work reported in this paper.

Acknowledgements

The authors acknowledge the French ANR agency for its financial support.

Appendix A. Supporting information

Supplementary data associated with this article can be found in the online version at doi:10.1016/j.apcatb.2021.121051.

References

[1] T. Werpy, P.N.N. Laboratory, G. Petersen, N.R.E. Laboratory, Top Value Added Chemicals from Biomass: Volume I–Results of Screening for Potential Candidates from Sugars and Synthesis Gas, n.d., 76.
[2] A. Démolis, N. Essayem, F. Rataboul, Synthesis and applications of alkyl levulinates, ACS Sustain. Chem. Eng. 2 (2014) 1338–1352, https://doi.org/10.1021/sc500082n.
[3] D.J. Hayes, S. Fitzpatrick, M.H.B. Hayes, J.R.H. Ross, The biofine process–production of levulinic acid, furfural, and formic acid from lignocellulosic feedstocks, in: B. Kamm, P.R. Gruber, M. Kamm (Eds.), Biorefineries-Ind. Process. Prod., Wiley-VCH Verlag GmbH, Weinheim, Germany, 2005, pp. 139–164, https://doi.org/10.1002/9783527619849.ch7.
[4] B. Girisuta, Levulinic Acid from Lignocellulosic Biomass, University of Groningen, 2007.
[5] H. Qu, B. Liu, G. Gao, Y. Ma, Y. Zhou, H. Zhou, L. Li, Y. Li, S. Liu, Metal-organic framework containing Brønsted acidity and Lewis acidity for efficient conversion glucose to levulinic acid, Fuel Process. Technol. 193 (2019) 1–6, https://doi.org/10.1016/j.fuproc.2019.04.035.
[6] Y. Liu, H. Li, J. He, W. Zhao, T. Yang, S. Yang, Catalytic conversion of carbohydrates to levulinic acid with mesoporous niobium-containing oxides, Catal. Commun. 93 (2017) 20–24, https://doi.org/10.1016/j.catcom.2017.01.023.
[7] R.L. De Souza, H. Yu, F. Rataboul, N. Essayem, 5-hydroxymethylfurfural (5-HMF) production from hexoses: limits of heterogeneous catalysis in hydrothermal conditions and potential of concentrated aqueous organic acids as reactive solvent system, Challenges 3 (2012) 212–232, https://doi.org/10.3390/challe3020212.
[8] Q. Hou, X. Qi, M. Zhen, H. Qian, Y. Nie, C. Bai, S. Zhang, X. Bai, M. Ju, Biorefinery roadmap based on catalytic production and upgrading 5-hydroxymethylfurfural, Green Chem. 23 (2021) 119–231, https://doi.org/10.1039/D0GC02770G.
[9] X. Qi, M. Watanabe, T.M. Aida, R.L. Smith, Catalytical conversion of fructose and glucose into 5-hydroxymethylfurfural in hot compressed water by microwave heating, Catal. Commun. 9 (2008) 2244–2249, https://doi.org/10.1016/j.catcom.2008.04.025.
[10] Q. Hou, M. Zhen, W. Li, L. Liu, J. Liu, S. Zhang, Y. Nie, C. Bai, X. Bai, M. Ju, Efficient catalytic conversion of glucose into 5-hydroxymethylfurfural by aluminum oxide in ionic liquid, Appl. Catal. B Environ. 253 (2019) 1–10, https://doi.org/10.1016/j.apcatb.2019.04.003.
[11] K. Nakajima, R. Noma, M. Kitano, M. Hara, Selective glucose transformation by titania as a heterogeneous Lewis acid catalyst, J. Mol. Catal. Chem. 388–389 (2014) 100–105, https://doi.org/10.1016/j.molcata.2013.09.012.
[12] J.M. Carraher, C.N. Fleitman, J.-P. Tessonnier, Kinetic and mechanistic study of glucose isomerization using homogeneous organic Brønsted base catalysts in water, ACS Catal. 5 (2015) 3162–3173, https://doi.org/10.1021/acscatal.5b00316.
[13] R.O.L. Souza, D.P. Fabiano, C. Feche, F. Rataboul, D. Cardoso, N. Essayem, Glucose–fructose isomerisation promoted by basic hybrid catalysts, Catal. Today 195 (2012) 114–119, https://doi.org/10.1016/j.cattod.2012.05.046.
[14] W. Mackenzie, Ethylene Global Supply Demand Analytics Service, 2018. ⟨https://www.woodmac.com/news/editorial/ethylene-global-supply-demand-analytics-service/⟩, (Accessed 22 March 2021).
[15] WORLDBAL_Documentation.pdf, n.d. ⟨http://wds.iea.org/wds/pdf/WORLDBAL_Documentation.pdf⟩, (Accessed 22 March 2021).
[16] R. Batchu, V.V. Galvita, K. Alexopoulos, Tatyana S. Glazneva, H. Poelman, M.-F. Reyniers, G.B. Marin, Ethanol dehydration pathways in H-ZSM-5: insights from temporal analysis of products, Catal. Today 355 (2020) 822–831, https://doi.org/10.1016/j.cattod.2019.04.018.
[17] R. Suerz, K. Eränen, N. Kumar, J. Wärnå, V. Russo, M. Peurla, A. Aho, D. Yu. Murzin, T. Salmi, Application of microreactor technology to dehydration of bio-ethanol, Chem. Eng. Sci. 229 (2021), 116030, https://doi.org/10.1016/j.ces.2020.116030.
[18] W. Alharbi, E. Brown, E.F. Kozhevnikova, I.V. Kozhevnikov, Dehydration of ethanol over heteropoly acid catalysts in the gas phase, J. Catal. 319 (2014) 174–181, https://doi.org/10.1016/j.jcat.2014.09.003.
[19] D. Fan, D.-J. Dai, H.-S. Wu, Ethylene formation by catalytic dehydration of ethanol with industrial considerations, Materials 6 (2012) 101–115, https://doi.org/10.3390/ma6010101.
[20] G. Chen, S. Li, F. Jiao, Q. Yuan, Catalytic dehydration of bioethanol to ethylene over TiO2/γ-Al2O3 catalysts in microchannel reactors, Catal. Today 125 (2007) 111–119, https://doi.org/10.1016/j.cattod.2007.01.071.
[21] J.M. Jacobs, P.A. Jacobs, J.B. Uytterhoeven, Procédé d'obtention d'éthylène à partir d'éthanol, EP0175399A1, 1986. ⟨https://patents.google.com/patent/EP0175399A1/fr⟩, (Accessed 26 November 2021).
[22] L.M. Betts, F. Dappozze, C. Guillard, Understanding the photocatalytic degradation by P25 TiO2 of acetic acid and propionic acid in the pursuit of alkane production, Appl. Catal. Gen. 554 (2018) 35–43, https://doi.org/10.1016/j.apcata.2018.01.011.
[23] J. Ambigadevi, P. Senthil Kumar, D.-V.N. Vo, S. Hari Haran, T.N. Srinivasa Raghavan, Recent developments in photocatalytic remediation of textile effluent using semiconductor based nanostructured catalyst: a review, J. Environ. Chem. Eng. 9 (2021), 104881, https://doi.org/10.1016/j.jece.2020.104881.

[24] S. Helali, F. Dappozze, S. Horikoshi, T.H. Bui, N. Perol, C. Guillard, Kinetics of the photocatalytic degradation of methylamine: influence of pH and UV-A/UV-B radiant fluxes, J. Photochem. Photobiol. Chem. 255 (2013) 50–57, https://doi.org/10.1016/j.jphotochem.2012.12.022.
[25] M. de, O. Melo, L.A. Silva, Photocatalytic production of hydrogen: an innovative use for biomass derivatives, J. Braz. Chem. Soc. (2011), https://doi.org/10.1590/S0103-50532011000800002.
[26] I. Barba-Nieto, K.C. Christoforidis, M. Fernández-García, A. Kubacka, Promoting H2 photoproduction of TiO2-based materials by surface decoration with Pt nanoparticles and SnS2 nanoplatelets, Appl. Catal. B Environ. 277 (2020), 119246, https://doi.org/10.1016/j.apcatb.2020.119246.
[27] H. Bahruji, M. Bowker, P.R. Davies, L.S. Al-Mazroai, A. Dickinson, J. Greaves, D. James, L. Millard, F. Pedrono, Sustainable H2 gas production by photocatalysis, J. Photochem. Photobiol. Chem. 216 (2010) 115–118, https://doi.org/10.1016/j.jphotochem.2010.06.022.
[28] H. Zhao, C.-F. Li, X. Yong, P. Kumar, B. Palma, Z.-Y. Hu, G. Van Tendeloo, S. Siahrostami, S. Larter, D. Zheng, S. Wang, Z. Chen, M.G. Kibria, J. Hu, Coproduction of hydrogen and lactic acid from glucose photocatalysis on band-engineered Zn1-xCdxS homojunction, IScience 24 (2021), 102109, https://doi.org/10.1016/j.isci.2021.102109.
[29] L. Zhang, W. Wang, S. Zeng, Y. Su, H. Hao, Enhanced H2 evolution from photocatalytic cellulose conversion based on graphitic carbon layers on TiO2/NiOx, Green Chem. 20 (2018) 3008–3013, https://doi.org/10.1039/C8GC01398E.
[30] B. Zhou, J. Song, Z. Zhang, Z. Jiang, P. Zhang, B. Han, Highly selective photocatalytic oxidation of biomass-derived chemicals to carboxyl compounds over Au/TiO2, Green Chem. 19 (2017) 1075–1081, https://doi.org/10.1039/C6GC03022J.
[31] M. Bellardita, E.I. García-López, G. Marcì, L. Palmisano, Photocatalytic formation of H2 and value-added chemicals in aqueous glucose (Pt)-TiO2 suspension, Int. J. Hydrog. Energy 41 (2016) 5934–5947, https://doi.org/10.1016/j.ijhydene.2016.02.103.
[32] I. Abdouli, M. Eternot, F. Dappozze, C. Guillard, N. Essayem, Comparison of hydrothermal and photocatalytic conversion of glucose with commercial TiO2: superficial properties-activities relationships, Catal. Today (2020), https://doi.org/10.1016/j.cattod.2020.03.040.
[33] S.E. Davis, B.N. Zope, R.J. Davis, On the mechanism of selective oxidation of 5-hydroxymethylfurfural to 2,5-furandicarboxylic acid over supported Pt and Au catalysts, Green Chem. 14 (2012) 143–147, https://doi.org/10.1039/C1GC16074E.
[34] A. Abbadi, H. van Bekkum, Effect of pH in the Pt-catalyzed oxidation of D-glucose to d-gluconic acid, J. Mol. Catal. Chem. 97 (1995) 111–118, https://doi.org/10.1016/1381-1169(94)00078-6.
[35] M. Liu, X. Jin, G. Zhang, Q. Xia, L. Lai, J. Wang, W. Zhang, Y. Sun, J. Ding, H. Yan, C. Yang, Bimetallic AuPt/TiO2 catalysts for direct oxidation of glucose and gluconic acid to tartaric acid in the presence of molecular O_2, ACS Catal. 10 (2020) 10932–10945, https://doi.org/10.1021/acscatal.0c02238.
[36] P. Qi, S. Chen, J. Chen, J. Zheng, X. Zheng, Y. Yuan, Catalysis and reactivation of ordered mesoporous carbon-supported gold nanoparticles for the base-free oxidation of glucose to gluconic acid, ACS Catal. 5 (2015) 2659–2670, https://doi.org/10.1021/cs502093b.
[37] K. Dussan, B. Girisuta, M. Lopes, J.J. Leahy, M.H.B. Hayes, Conversion of hemicellulose sugars catalyzed by formic acid: kinetics of the dehydration of D-xylose, L-arabinose, and D-glucose, ChemSusChem 8 (2015) 1411–1428, https://doi.org/10.1002/cssc.201403328.
[38] J.-M. Herrmann, Heterogeneous photocatalysis: fundamentals and applications to the removal of various types of aqueous pollutants, Catal. Today 53 (1999) 115–129, https://doi.org/10.1016/S0920-5861(99)00107-8.
[39] H.S. Kim, S.-K. Kim, G.-T. Jeong, Catalytic conversion of glucose into levulinic and formic acids using aqueous Brønsted acid, J. Ind. Eng. Chem. 63 (2018) 48–56, https://doi.org/10.1016/j.jiec.2018.01.038.
[40] F. Conti, S. Begotti, F. Ippolito, Procédé De Production D′acide Lévulinique, 2018. ⟨https://patentscope.wipo.int/search/fr/detail.jsf?docId=WO2018235012&tab=PCTDESCRIPTION⟩, (Accessed 26 May 2021).
[41] N.A.S. Ramli, N.A.S. Amin, Kinetic study of glucose conversion to levulinic acid over Fe/HY zeolite catalyst, Chem. Eng. J. 283 (2016) 150–159, https://doi.org/10.1016/j.cej.2015.07.044.
[42] N.A.S. Ramli, N.A.S. Amin, Fe/HY zeolite as an effective catalyst for levulinic acid production from glucose: characterization and catalytic performance, Appl. Catal. B Environ. 163 (2015) 487–498, https://doi.org/10.1016/j.apcatb.2014.08.031.
[43] N. Ya'aini, N.A.S. Amin, S. Endud, Characterization and performance of hybrid catalysts for levulinic acid production from glucose, Microporous Mesoporous Mater. 171 (2013) 14–23, https://doi.org/10.1016/j.micromeso.2013.01.002.
[44] H. Kitajima, Y. Higashino, S. Matsuda, H. Zhong, M. Watanabe, T.M. Aida, R. L. Smith, Isomerization of glucose at hydrothermal condition with TiO2, ZrO2, CaO-doped ZrO2 or TiO2-doped ZrO2, Catal. Today 274 (2016) 67–72, https://doi.org/10.1016/j.cattod.2016.01.049.
[45] T.M. Aida, A. Ikarashi, Y. Saito, M. Watanabe, R.L. Smith, K. Arai, Dehydration of lactic acid to acrylic acid in high temperature water at high pressures, J. Supercrit. Fluids 50 (2009) 257–264, https://doi.org/10.1016/j.supflu.2009.06.006.
[46] N. Sobuś, I. Czekaj, Lactic acid conversion into acrylic acid and other products over natural and synthetic zeolite catalysts: theoretical and experimental studies, Catal. Today (2021), https://doi.org/10.1016/j.cattod.2021.10.021.
[47] X. Zhang, L. Lin, T. Zhang, H. Liu, X. Zhang, Catalytic dehydration of lactic acid to acrylic acid over modified ZSM-5 catalysts, Chem. Eng. J. 284 (2016) 934–941, https://doi.org/10.1016/j.cej.2015.09.039.
[48] Y. Matsuura, A. Onda, K. Yanagisawa, Selective conversion of lactic acid into acrylic acid over hydroxyapatite catalysts, Catal. Commun. 48 (2014) 5–10, https://doi.org/10.1016/j.catcom.2014.01.009.
[49] D.J. Titheridge, M.A. Barteau, H. Idriss, Reaction of acrylic acid on TiO2(001) single crystal surfaces. Evidence of different pathways for vinyl and carboxyl groups, Langmuir 17 (2001) 2120–2128, https://doi.org/10.1021/la000931o.